Chapter 4

EXPLORING THE INTERPHASE AND ITS IMPACT ON ELECTRO-THERMAL PROPERTIES

4.1 INTRODUCTION

Polymer nanocomposites offer unprecedented material properties, which are widely attributed to a high proportion of interphase generated between the matrix and filler material. However, the mechanism by which interphases forms in polymer nanocomposites remains elusive. This chapter presents a thorough investigation of the interphase development in epoxy alumina nanocomposites and its relationship to their dielectric and thermal properties. To investigate interphase formation, three different types of samples were synthesized viz. pure epoxy, nanocomposites (without surface treatment of fillers), and nanocomposites with surface treatment of fillers (with surface treatment of fillers). Dielectric properties measurements are performed on synthesized samples, including ac dielectric strength, complex permittivity, and dc conductivity. Additionally, thermogravimetric analysis (TGA) and differential scanning calorimetry (DSC) is used to determine the thermal characteristics of nanocomposites. Finally, FTIR spectroscopy is used to investigate how interphases are formed as a result of chemical interaction between two constituent phases.

4.2 EXPERIMENTAL

4.2.1 Sample Preparation and Dispersion Analysis

A procedure described in Chapter 2 is used to prepare dielectric samples (section 2.2.3). The literature has proven that filler dispersion plays a critical role in the changing of characteristics in PNC. Thus, in this study the dispersion of fillers in the polymer matrix is initially investigated using FESEM. Figure 4.1a and 4.1b illustrate typical SEM images of nanocomposites with a filler content of (1 vol. %) that were synthesized respectively using untreated and surface-treated nanoparticles. The nanoparticles are seen to be disseminated adequately in the base resin.

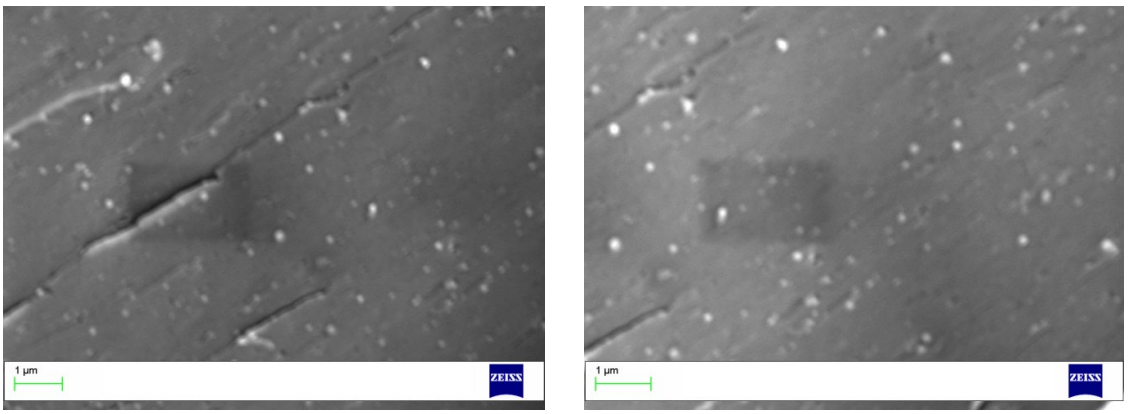

(a) (b)

Figure 4.1 SEM images of nanocomposites (a) with untreated nanofillers (b) with surface treated nanofillers

However, the SEM images given above provide only a qualitative assessment of dispersion homogeneity. The degree of dispersion and the extent of agglomeration can be quantified using the method provided in Chapter 2 (section 2.3). SEM images are initially digitized in this work using MATLAB's image processing toolbox, which supports IMREAD compatible images. This tool box enables users to graphically identify the origin, the reference scale (the scale bar on the image), and the quantity of

data points to be selected graphically from appropriate areas on the image. Figure 4.2 depicts a digitized image revealing the nanoparticles' center coordinates. The average interparticle distance can be used to determine the quality of filler dispersion and the level of agglomeration. Significant divergence from the reference (anticipated value) value for the estimated inter-particle distance indicates particle aggregation. The average inter-particle distance is estimated using micrographs of five randomly selected samples from each specimen. The inter-particle distance reference value is calculated on the assumption that the unit cell generated by uniformly dispersed nanoparticles resembles a simple cubic lattice structure.

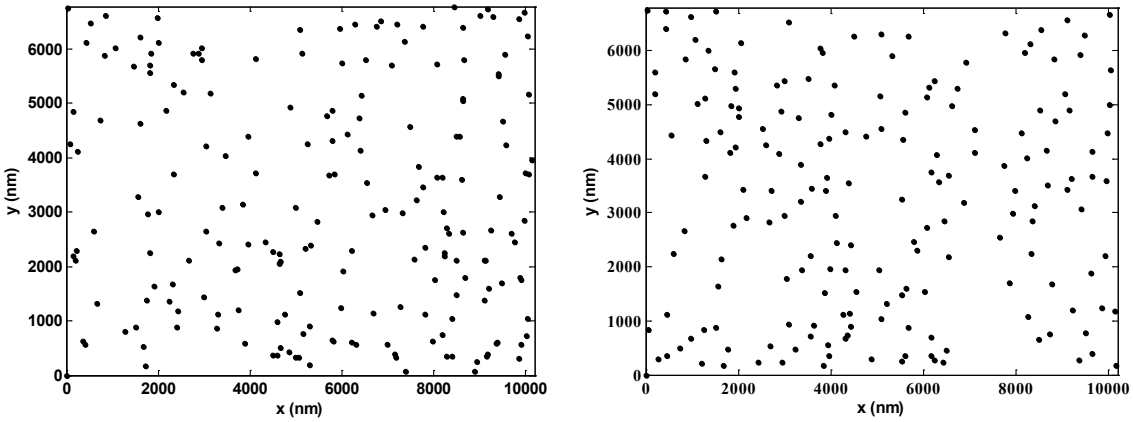

(a) (b)

Figure 4.2 Digitized images indicating center coordinates of nanoparticles (a) with untreated nanofillers (b) with surface treated nanofillers

The reference value and estimated interparticle distance for various filler concentrations are shown in Table 4.1. For both forms of nanocomposites (i.e., nanocomposites made with untreated and surface-treated nanofillers), the maximum filler concentrations at which the dispersion quality is almost comparable is 1 vol. %. As a result, this investigation is conducted at a filler concentration of 1 vol. %.

Table 4.1 Quantification of nano-filler dispersion in nanocomposites

Filler concentrations (by volume)	**Reference value of inter-particle distance (D_r)**	**Estimated inter-particle distance in nanocomposite formed with untreated nanoparticles (D_{a1})**	**Estimated inter-particle distance in nanocomposite formed with surface treated nanoparticles (D_{a2})**	**Degree of dispersion non-uniformity in nanocomposite formed with untreated nanoparticles (D_r/D_{a1})**	**Degree of dispersion non-uniformity in nanocomposite formed with surface treated nanoparticles (D_r/D_{a2})**
0.5 vol.%	231 nm	242 nm	241 nm	0.955	0.960
1 vol.%	***187 nm***	***199 nm***	***198 nm***	***0.940***	***0.954***
1.5 vol.%	163 nm	185 nm	173 nm	0.880	0.940
2 vol.%	148 nm	190 nm	161 nm	0.780	0.920

4.2.2 X-Ray Diffraction (XRD) Analysis

XRD pattern of epoxy resin is shown in Figure 4.3a. A broad peak is observed due to the amorphous nature of the material. XRD graph of alumina nanoparticles is shown in Figure 4.3b, where different characteristic peaks are present. The effect of nano-alumina inclusion is clearly observable in the XRD pattern of epoxy nanocomposite as seen in Figure 4.3c.

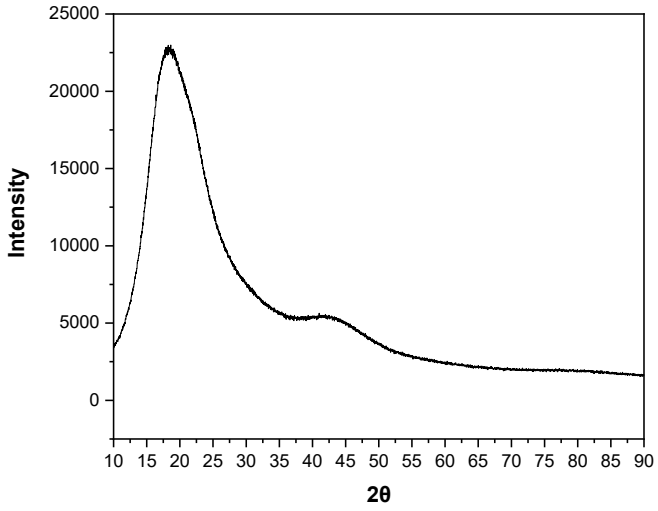

(a)

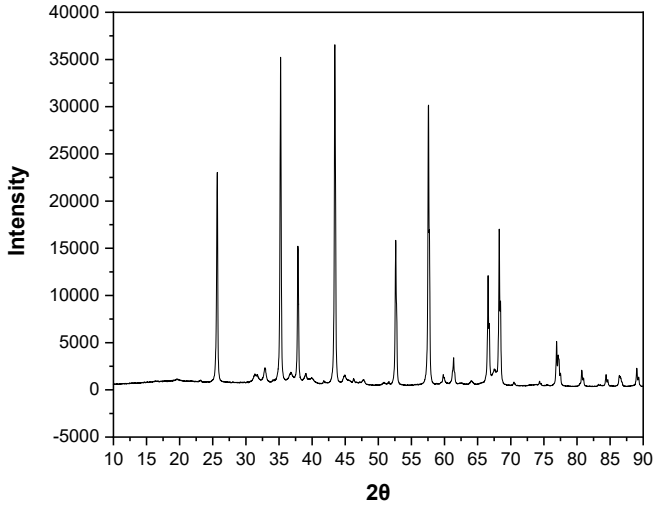

(b)

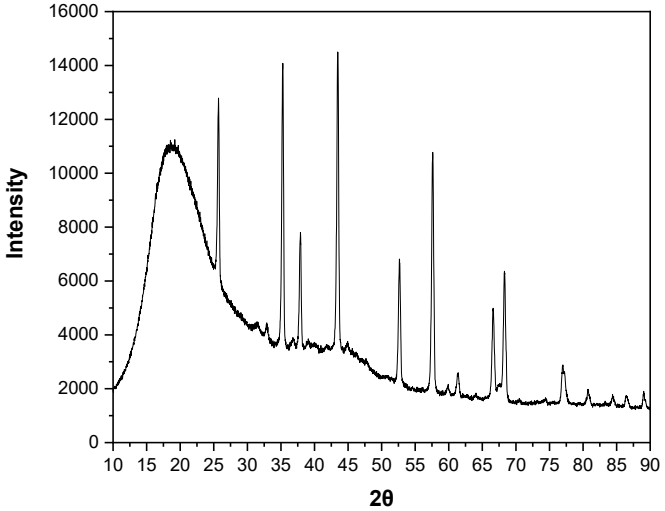

(c)

Figure 4.3 XRD pattern of: (a) epoxy (b) alumina nanoparticle (c) epoxy alumina nanocomposites

4.2.3 Dielectric Properties Measurements

4.2.3.1 Measurements of AC Dielectric strength

AC breakdown strength measurement is carried out as discussed in chapter 3, section 3.2.1. Breakdown data are analyzed using 2 parameter Weibull distributions. Figure 4.4 shows the plots for all three kinds of samples. Scale and shape parameters estimated from the Weibull plot are shown in Table 4.2.

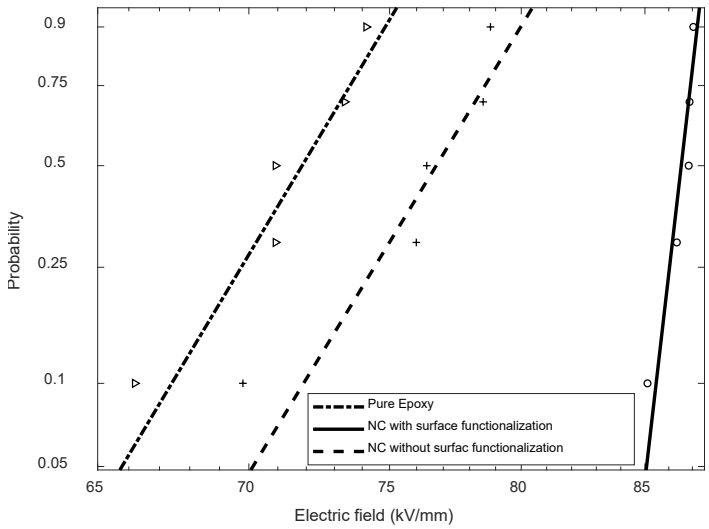

Figure 4.4 Weibull probability plot for the short-term AC dielectric strength of epoxy and nanocomposites.

Table 4.2 Weibull parameters (α and β)

Specimen	**Weibull Parameters**	
	Scale parameter (α)	Shape parameter (β)
Neat epoxy	72.35	34.35
Epoxy nanocomposites (without surface functionalized nanofillers)	76.19	20.19
Epoxy nanocomposites (with surface functionalized nanofillers)	86.74	95.91

Nanocomposites have greater resilience to AC stress than pure epoxy. At the moment, the exact process by which dielectric strength is increased is unknown. However, it is possible that the nanoparticles act as a trap for charge carriers, thereby alleviating internal ionization or molecular dissociation [2]. Several further characterizations have been performed in the following sections to gain a better understanding of the ac breakdown features of all three types of samples.

4.2.3.2 DC Conductivity

DC conductivity measurements are made in the same manner as detailed in Chapter 3. Figure 4.5 depicts the polarisation current plot. Table 4.3 shows the value of dc conductivities measured at a 2 kV/mm applied electric field. Epoxy nanocomposites made with untreated nanofillers have a slightly higher dc conductivity than pure epoxy. On the other hand, nanocomposites synthesized with surface functionalized nanofillers have a lower dc conductivity than pure epoxy resin. The little increase in dc conductivity of composites formed with untreated nanofillers could be attributable to the presence of ionic contaminants in the composites [3].

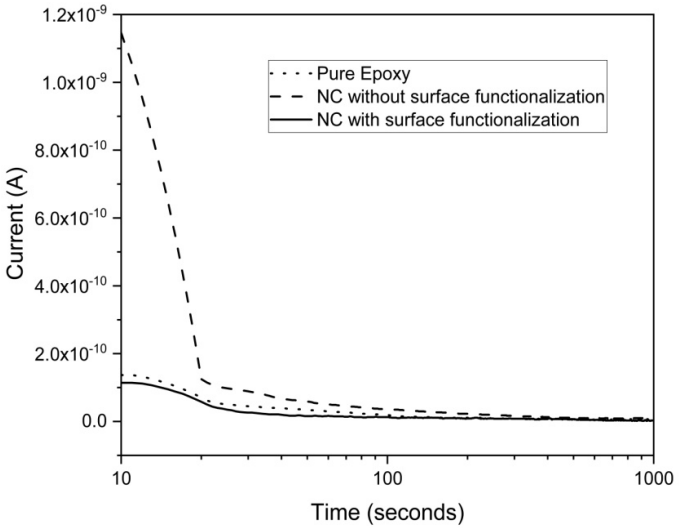

Figure 4.5 Polarization current at an applied electric field of 2 kV/mm

Table 4.3 Measured DC conductivity at an applied electric field of 2 kV/mm

Specimen	DC conductivity (S/m)
Pure Epoxy	1.98E-14 ± 1%
Epoxy nanocomposites (without surface functionalized nanofillers)	5.09E-14 ± 1%
Epoxy nanocomposites (with surface functionalized nanofillers)	1.92E-14 ± 1%

To further elucidate the decrease in dc conductivity of nanocomposites due incorporation of surface-treated nanofillers, the following section performs several additional characterizations.

4.2.3.3 Dielectric spectroscopy

The complex permittivity of dielectric samples has been measured using broad band dielectric spectroscopy over a wide frequency range. The measurements are made in the way described in Chapter 3. Figure 4.6 illustrates the variation of the real and imaginary parts of complex relative permittivity as a function of frequency. Table 4.4 shows the relative permittivity and dielectric loss factor at 50 Hz.

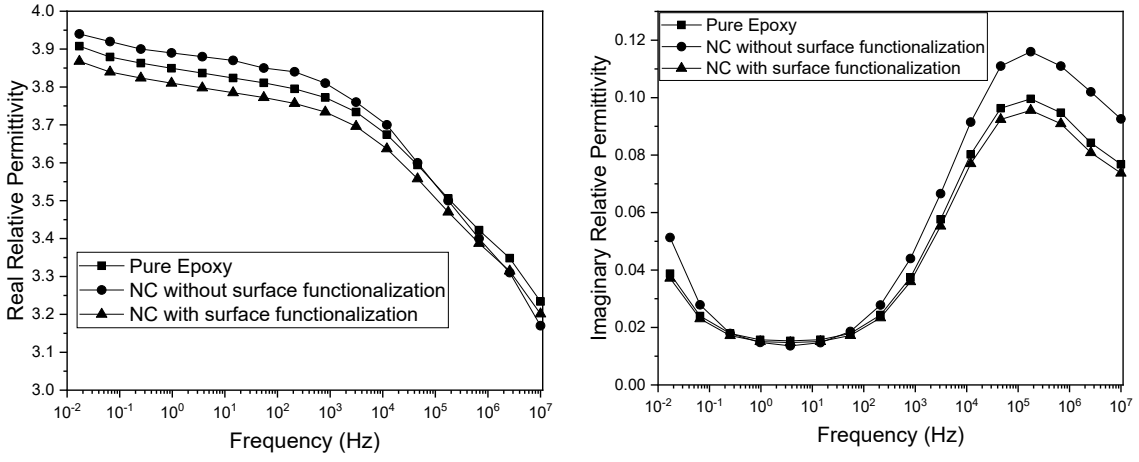

(a) (b)

Figure 4.6 Complex relative permittivity (a) real part (εr′) (b) imaginary part (εr″)

Table 4.4 Measured relative permittivity and loss tangent (tanδ) at 50Hz

Specimen	Relative Permittivity		Loss tangent (tanδ)
	Real part (ε_r')	Imaginary part (ε_r'')	
Pure epoxy	3.81	0.0179	0.00470
Epoxy nanocomposites (without surface functionalized nanofillers)	3.85	0.0186	0.00483
Epoxy nanocomposites (with surface functionalized nanofillers)	3.77	0.0172	0.00456

The complex permittivity and dielectric loss tangent (tanδ) for nanocomposites formed with surface treated nanofillers show distinct characteristics with respect to both pure epoxy and nanocomposites (synthesized with untreated nanofillers). The anomalous dielectric response of nanocomposites suggests the existence of a hitherto unknown phenomena occurring exclusively in nanocomposites manufactured using surface-treated nanofillers.

4.2.4 Thermogravimetric analysis (TGA)

The TGA technique was used to determine the influence of nanofiller inclusion on the thermal stability of the base resin. The TGA graphs of pure epoxy and nanocomposites are displayed in Figure 4.7, and 20% degradation temperature of pure epoxy and nanocomposites is given in Table 4.5.

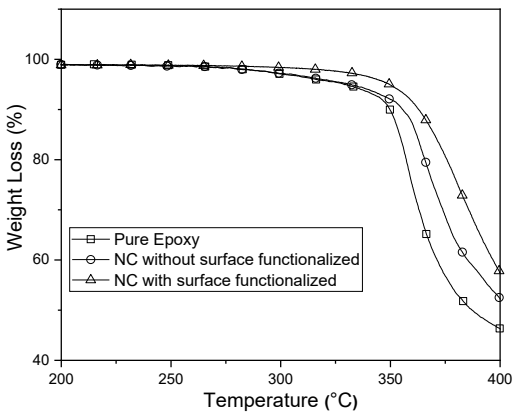

Figure 4.7 TGA plots for epoxy and nanocomposites

Table 4.5 Degradation temperature of pure epoxy and nanocomposites

Samples	Degradation Temperature ($T_{20\%}$) (°C)
Pure epoxy	357.27 ± 0.5%
NC with untreated NP	365.72 ± 0.5%
NC with surface treated NP	375.94 ± 0.5%

A 20% degradation temperature signifies the temperature at which the weight loss of the sample is 20%. It is evident from the experimental data that nanocomposites are thermally more stable than neat epoxy resin.

4.2.5 Differential scanning calorimetry (DSC)

The effect of nano-filler inclusion on the glass transition (Tg) temperature of polymer was investigated using DSC. Figure 4.8 illustrates the DSC graphs of pure epoxy and nanocomposites, and Table 4.6 shows the glass transition temperatures (Tg) of pure epoxy and nanocomposites. As illustrated in Table 4.6, the glass transition temperature has increased slightly.

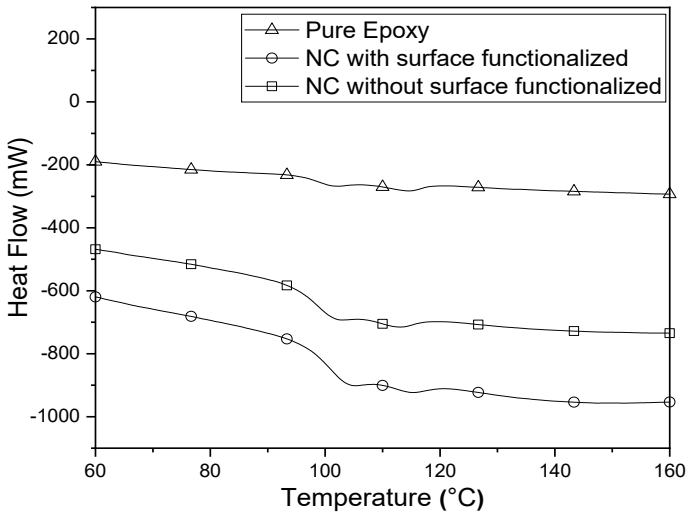

Figure 4.8 DSC graph of Nanocomposites

Table 4.6 Glass transition temperature (Tg) data of pure epoxy and Nanocomposites

Samples	Glass transition temperature (T_g) (°C)
Pure epoxy	98.7 ± 0.1%
NC without surface functionalized nanoparticle	99.4 ± 0.1%
NC with surface functionalized nanoparticle	102.1 ± 0.1%

The glass transition temperature of nanocomposites prepared with surface functionalized nanofillers is greater than that of nanocomposites prepared with as-received (or untreated) nanofillers.

The cause of the two types of nanocomposites' varied behavior will be elucidated using data obtained from multiple material characterization techniques, and comprehensive analysis will be provided in the next section.

4.3 GENESIS OF INTERPHASE AND ITS RELATIONSHIP WITH MATERIAL PROPERTIES

Experimental data on TGA indicates that nanocomposites are thermally more stable than neat epoxy resin. AC dielectric strength of base polymer is improved through the inclusion of nanofillers. However, improvement is relatively more striking if nanocomposites are synthesized with surface-treated nanofillers. Experimental findings on dielectric spectroscopy and conduction current measurements are even more intriguing. The complex permittivity of nanocomposites synthesized with as received nanofillers is more than that of neat epoxy. On the other hand, nanocomposites synthesized with surface-treated nanofillers exhibit lower complex permittivity than that of neat epoxy. It is indeed a thought-provoking situation where effective permittivity of two-phase dielectric mixture is lower than the permittivity of both constituent phases

(i.e., filler and matrix). Similarly, the dc conductivity of nanocomposites formed with surface-treated nanofillers is lower than base polymer. Anomalous dielectric responses disported by nanocomposites signalize the co-existence of third phase along with filler and matrix. A systematic investigation is carried out to understand the rationale behind this distinctive behavior of nanocomposites formed with surface-treated nanofillers.

Polymerization process begins by reaction of epoxide group of base resin with the amine group of the hardener. In this reaction, the epoxide group is attacked by the primary amine group as shown in Figure 4.9. The combination of the epoxide group and the primary amine group creates a secondary amine group and a pendant hydroxyl group, these results in disappearing of the epoxide group. In the second step, the remaining hydrogen of the secondary amine group reacts with another epoxide group of the resin to form a branch point. Eventually, the opening of the epoxide group of the epoxy resin and formation of branches develops a three-dimensional molecular network of high molecular weight thermosetting polymer [89]. This chemical interaction between base polymer and curing agent is verified using FTIR spectroscopy. Figure 4.10 shows FTIR spectra of uncured epoxy resin, hardener, and cured epoxy. FTIR spectra of uncured epoxy resin show two peaks at wave numbers 970.16 and 915.74 cm^{-1}. These peaks confirm the presence of epoxide group in uncured epoxy resin. On completion of curing process, the characteristic peak at 915.74 $cm.^{-1}$ disappears, and the intensity of characteristic band (C-N bond) at 1085 $cm.^{-1}$ increases due to cross-linking.

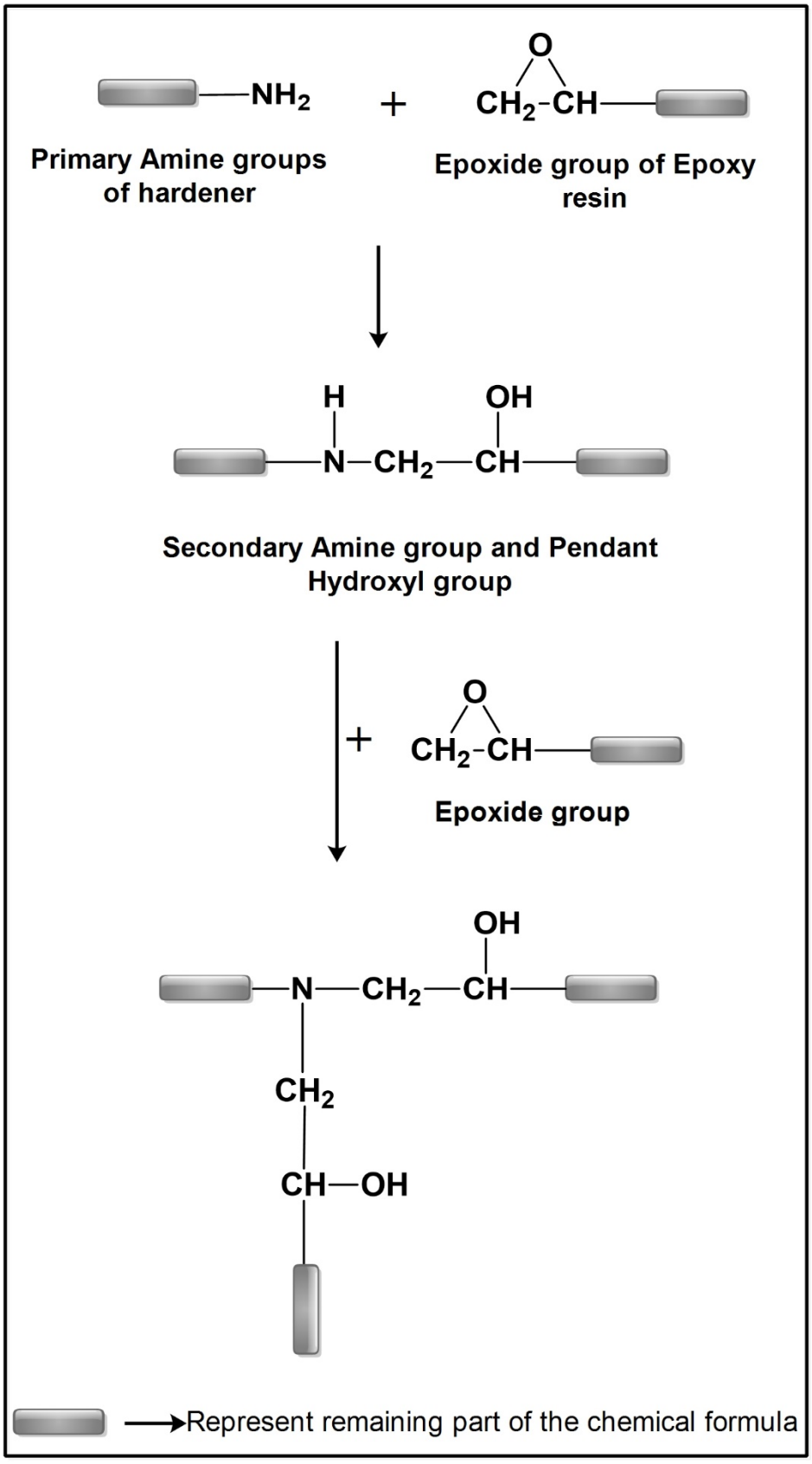

Figure 4.9 Flow diagram on curing process of epoxy resin

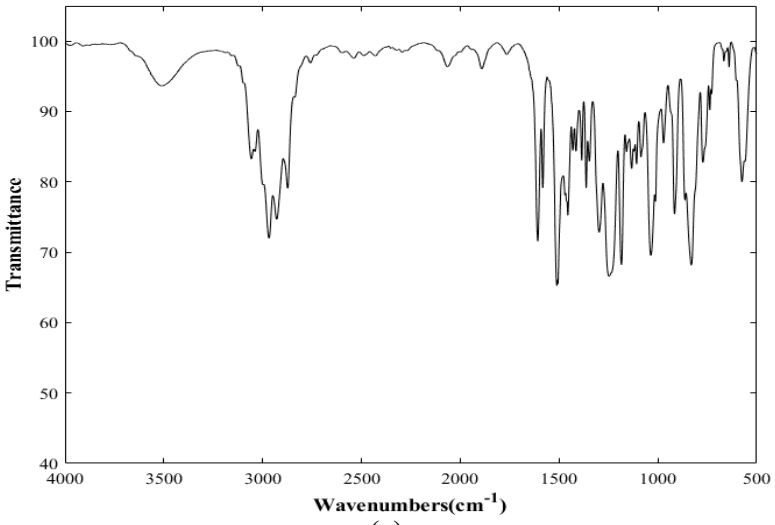

(a)

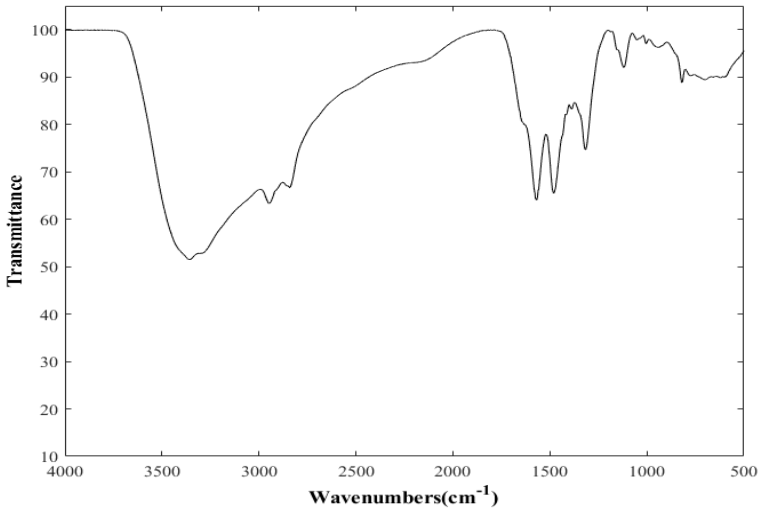

(b)

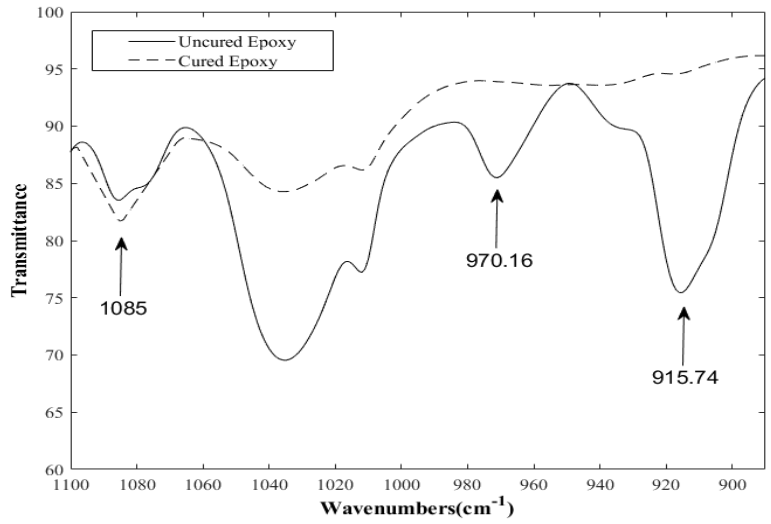

(c)

Figure 4.10 FTIR spectra (a) uncured epoxy (b) hardener (c) cured epoxy

The intrinsic nature of inorganic oxides fillers does not make them compatible with an organic resin. In an endeavor to make them interactive with the base resin, they are pre-processed using a coupling agent following a process described in [84]. The coupling agent chemically bridges the particle surface with the base resin. Effective coupling is possible if the coupling agent has a chemical structure whose head is compatible with particle surface, and the tail has a functional group that reacts with base resin during curing. Figure 4.11 shows the chemical structure of 3-glycidoxypropyl trimethoxysilane (GPS) with functional group present on both sides (head and tail). The surface functionalization of nanoparticles takes place by chemical reaction between the hydroxyl groups present on the surface of nanoparticles and the methoxy groups of the GPS molecules. The organofunctional group present on another side of the GPS molecule reacts with the epoxy resin through cross-linker during curing [90], [91]. Surface functionalization of alumina nanoparticles using GPS and different stages involved is shown in Figure 4.12. The methoxy groups of the GPS molecule convert into the hydroxyl groups after the hydrolysis process, and then these hydroxyl groups react with the hydroxyl groups present on the surface of alumina nanoparticles and form a strong Si-O-Al bond [84]. FTIR spectroscopy is carried out to justify the surface functionalization process described above. Figure 4.13a shows FTIR spectra of untreated alumina nanoparticles. A broad peak at 3450.03 cm^{-1} represents the hydroxyl groups present on the surface of the untreated alumina nanoparticles [92], [93]. The FTIR graph of silane-treated alumina nanoparticles in Figure 4.13c shows an extra broad peak at 1110.34 cm^{-1}. This peak (at 1110.34 cm^{-1}) is missing in the FTIR spectra of untreated alumina nanoparticles. The broad peak at 1110.34 cm^{-1} is attributed to the formation of Si–O–Al bond.

The detail of peak in FTIR spectra of as received nanofiller is given below:

- 3450.03 cm^{-1} corresponds to the stretching vibration of the OH group.

The details of peaks in FTIR spectra of silane functionalized nanofiller are given below:

- 3452.92 cm^{-1} corresponds to the stretching vibration of the OH group.
- 2942.35 cm^{-1} and 2841.11 cm^{-1} corresponds to the symmetrical and asymmetrical stretching vibration of the CH_3 and CH_2 groups.
- 1466.11 cm^{-1} corresponds to the scissoring deformation and asymmetrical deformation vibrations of the CH_3 and CH_2 groups.
- 1110.34 cm^{-1} corresponds to asymmetrical Si-O stretching vibration of the Si-O-Al bond.

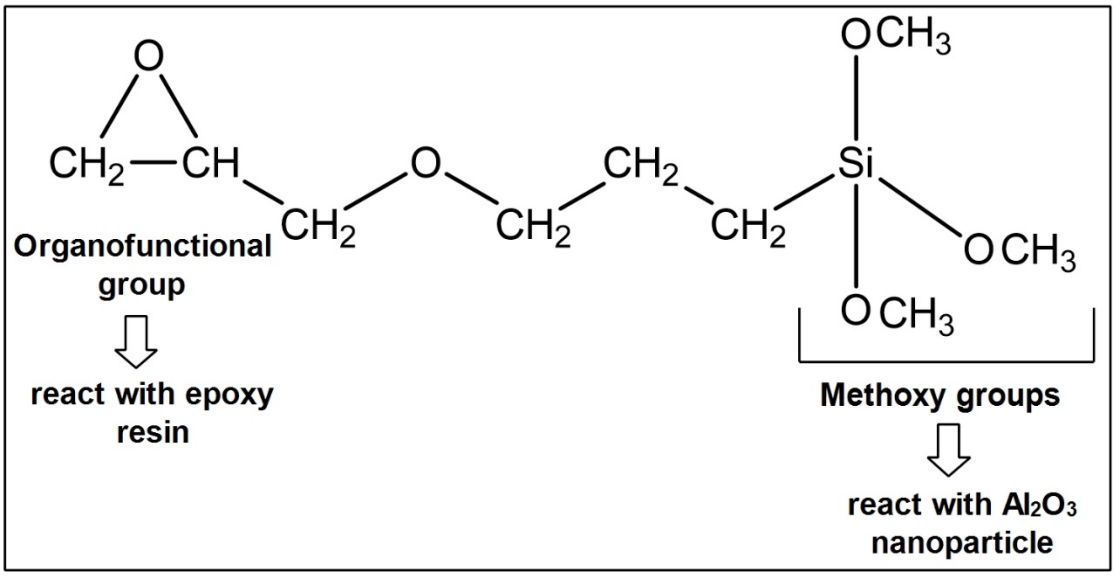

Figure 4.11 Chemical structure and reactive functional groups of GPS

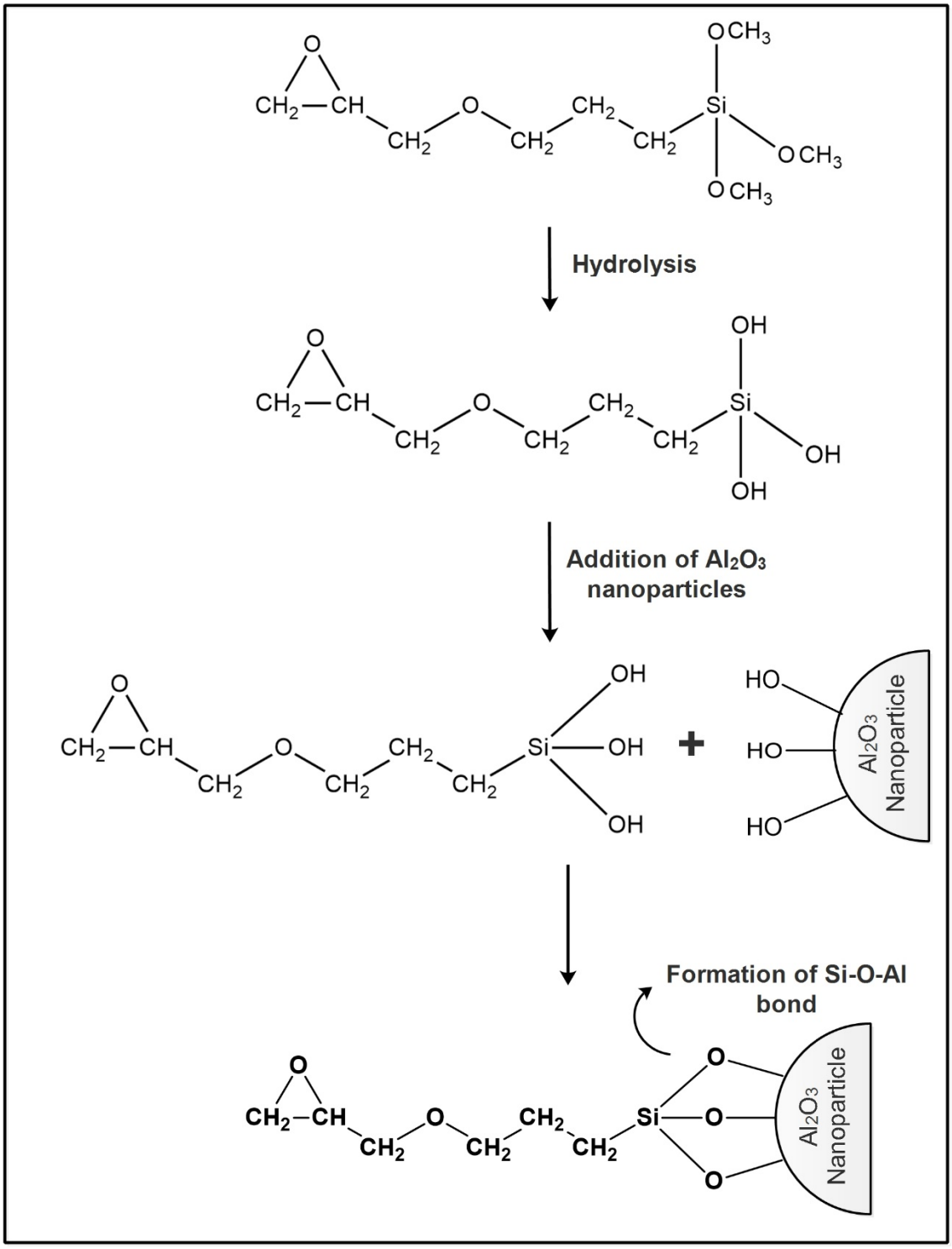

Figure 4.12 Schematic diagram to illustrate surface functionalization of alumina nanoparticles

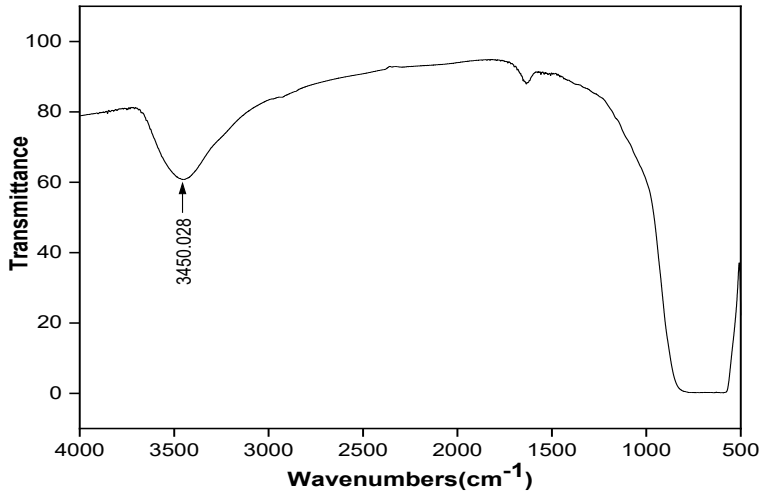

(a)

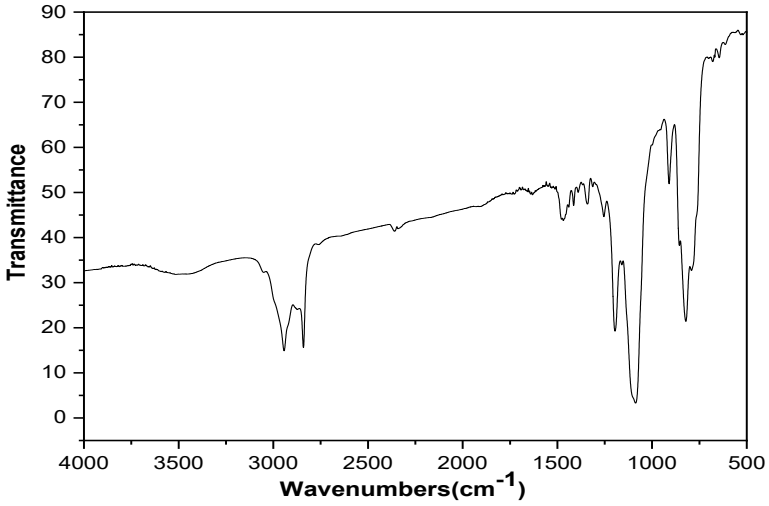

(b)

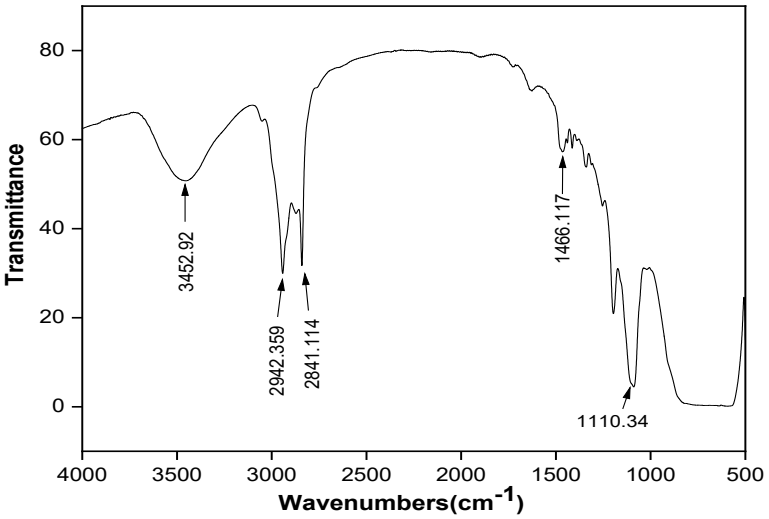

(c)

Figure 4.13 FTIR spectra of (a) as received nanofillers (b) GPS (c) surface treated nanofillers

At a filler content of 1 vol.%, nanofiller dispersion (with and without surface treatment) is nearly same (Table 4.1). Hence, it may be asserted that nanocomposites synthesized with surface functionalized nanofillers exhibit improved material properties solely due to enhanced interfacial interaction between particle and polymer matrix. Tanaka [94], [95] proposed a theoretical three-core model to understand the correspondence between interphase and material properties of polymer nanocomposites. The first layer (bonded layer) is bonded to both the filler and polymer. The second interfacial region consisting of polymer chains strongly bound to the first layer, and loosely coupled to the third layer. According to his proposed model, the improved dc conductivity of nanocomposites with surface-functionalized nanoparticles is due to the reduction in volume fraction of loose layer and increase in the volume fraction of the tightly bound immobile layer. Thus, the movement of ions in the tightly bound layer is restricted. Similarly, water-shell model proposed by Zou et al. [96] explained Quasi-DC behavior at low frequency in epoxy silica nanocomposites. They suggested that the dielectric properties of nanocomposites synthesized with surface functionalization nanofillers are less sensitive to humidity. Both aforementioned models are based on interfacial interaction between filler and matrix. However, a detailed experimental manifestation of physico-chemical interaction at interface is missing in these models. Raetzke et al. [97] introduced an interphase volume model on the basis of their experimental findings on silicone/SiO2 nanocomposites. In their model, it was assumed that the interphase formed around the nanoparticles is responsible for enhanced material properties. However, this model is salient on structure and properties of interfacial region.

This chemical interactive model is useful to explain various dielectric phenomena (electrical conduction, breakdown, complex permittivity etc.) in PNCs. Reduced dc conductivity due to enhanced interfacial interaction might cause homopolar

charge formation near electrodes. A shielding effect may prohibit charge injection from electrodes during the operation of dielectrics at elevated electric stress. Improved breakdown strength of nanocomposites may be attributed to the reduction in charge carrier injection and their participation in the breakdown process. Strong bonding of the polymer chain to the particle surface is expected to change its conformational motion and restrict dipole movement, which causes a reduction in complex permittivity of nanocomposites.

All dielectric measurements performed so far are under a uniform field environment where samples are electrically stressed for a short time frame. Further investigations are carried out to verify the impact of interfacial interaction on the long term performance of the nanodielectrics. In practice, dielectric materials used in electrical apparatus operate in non-uniform or divergent electric stress. Local stress intensification due to irregular surface or electrode geometry often gives rise to local discharge (or partial discharge). Energy dissipative process associated with partial discharge causes the treeing phenomenon in which eroded channels propagate along the volume of dielectrics. Electrical treeing is considered as one of the most important long-term failure mechanism. Thus, materials investigated in the present work are subjected to voltage endurance test to get the measure of their resistance against erosion under prolonged non-uniform ac stress. This test is conducted with needle plane geometry where needle (with tip radius of 5 μm) is embedded in the dielectric material and a distance of 3 mm is maintained between the needle tip and ground electrode. An ac voltage of 12 kV is continuously applied between the two electrodes till the sample fails. Test is conducted on five samples of each kind and average time to failure is recorded. The choice of applied voltage is based on electric field distribution computed

using COMSOL multi-physics (commercial finite element method-based software). Computed electric potential and field distribution is shown in Figure 4.14.

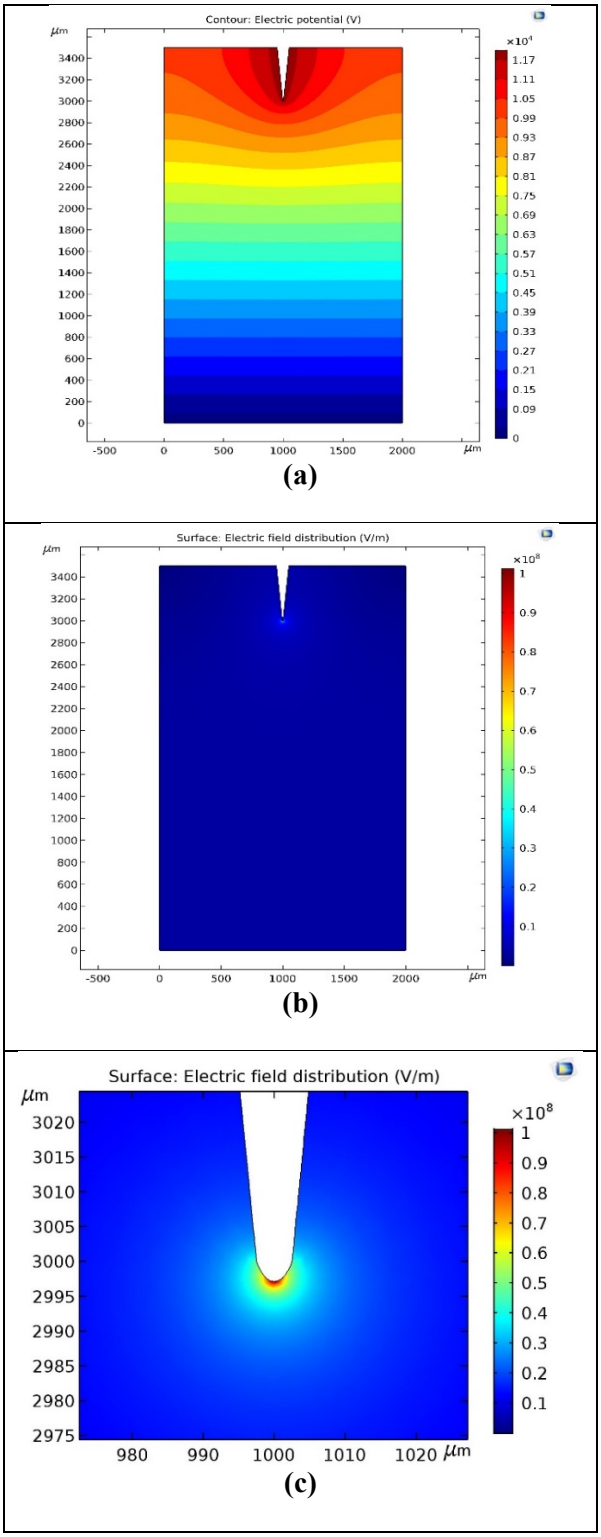

Figure 4.14 Electric potential and field distribution with needle-plane geometry (a) electric potential (b) electric field (c) electric field around needle tip (magnified view)

It may be noted that the electric field in a localized region around the needle tip is much higher than the breakdown strength of samples shown in Table 4.2. Hence, local material erosion is expected around the needle tip and cumulative erosion under prolonged application of ac stress leads to complete dielectric failure. Relative time to failure recorded for three kinds of samples is shown in Figure 4.15. The difference in failure time of three different kinds of samples may be attributed to the barrier effect introduced by nanofillers.

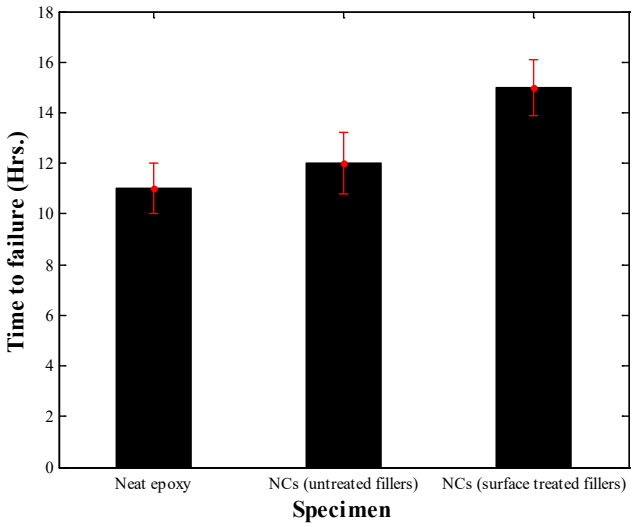

Figure 4.15 Time to failure (in Hrs.) during voltage endurance test

Schematic diagram (Figure 4.16) illustrates the barrier effect set forth by filler materials. Shortest path between the two electrodes through the weakest region is relatively shorter in pure epoxy than in nanocomposites. In nanocomposites, this path length is further extended if nanofillers are surface-functionalized due to the formation of interphase and strengthening of large proportion of epoxy resin around the fillers. Thus, the interphase seems to plays a crucial role in properties enhancement of nanocomposites.

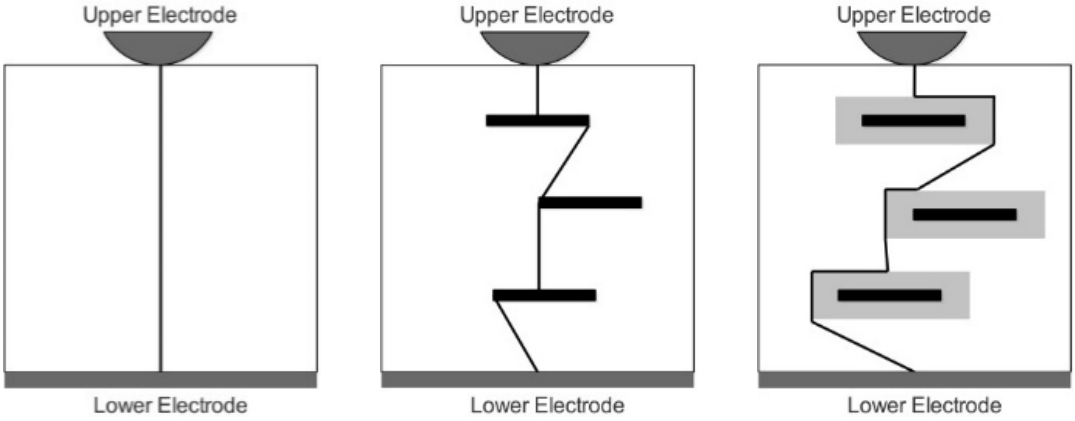

(a) (b) (c)

Figure 4.16 Barrier effect (a) pure epoxy (b) nanocomposites with untreated nanofillers (c) nanocomposites with surface treated nanofillers

4.4 SUMMARY

Experimental data bear witness to the fact that nanocomposites prepared with surface-treated nanofillers exhibit significantly different dielectric properties with respect to neat polymer and nanocomposites (formed with untreated nanofillers). Distinctive dielectric properties on account of filler surface treatment are attributed to the modified filler matrix interaction process, which culminates in the formation of the interphase. Comprehensive experimental work is presented to corroborate interphase formation and to provide viable inputs for tailoring the dielectric properties of PNCs through modified interfacial interaction (chemically or physically). Filler-matrix interaction is governed by adsorbed functional groups on the filler surface. The effect of filler matrix interaction may extend deep into the bulk. Thus, extent of interphase believed to shift percolation threshold, which in turn may modify many dielectric properties. Hence, qualitative analysis supplemented with quantitative assessment of interphase is of great importance to optimally manipulate different material properties. The next chapter covers quantitative interphase analysis.